NECKING BEHAVIOUR OF FLATTENED TUBULAR BRAIDED COMPOSITES

NECKING BEHAVIOUR OF FLATTENED TUBULAR BRAIDED COMPOSITES

Mayank Gautam[1], Prasad Potluri[2], Stephen Ogin[3], and Parshang Jain[4]

[1]Northwest Composite Centre, School of Materials, University of Manchester
Email: mayank.gautam@live.in

[2]Northwest Composite Centre, School of Materials, University of Manchester
Email: prasad.potluri@manchester.ac.uk

[3]Department of Mechanical Engineering Sciences, University of Surrey
Email: s.ogin@surrey.ac.uk

[4]School of Materials, University of Manchester,
Email: parshang.jain@student.manchester.ac.uk

Keywords: Braid Angle, Biaxial, Triaxial, Necking, and Specific Energy Absorption

ABSTRACT

This paper presents results on the effect of braid angle and tow boundary conditions on the stress-strain behaviour of carbon fibre and epoxy-based braided composites under tension for braid angles 35^0, 45^0 and 55^0. The specimens were produced by flattening the tubular braided sleeve during the preforming stage. The braid angle and tow continuity have a significant effect upon the pseudo-plastic and necking behaviour of the composites. Those specimens which showed extensive necking (all braid angles without cut edges and the 55^0 braid angle with cut edges) produced approximately the same specific energy absorption; specimens which showed either no, or very limited, pseudo-plasticity and necking, had low values of specific energy absorption. The addition of axial tow insertions can provide significant increases in the tensile mechanical properties (axial modulus and tensile strength) of the composites with continuous fibres while retaining significant pseudo-plasticity.

1 INTRODUCTION

Braiding is a textile preforming technique that offers dimensional stability and near-net shaped manufacturing capabilities, with the added advantage that braided composites often offer higher energy absorption properties as compared to metals due to the ability of composites to undergo large deformations (1). There is a need to design high performance and high energy absorbing materials and structures for civil, military and aerospace applications that could avoid catastrophic failure (2). Braided composites can exhibit higher energy absorption due to is multiple fibre fractures generated during the crushing process (3) moreover due to their crashworthiness and greater production speeds they are now being used now in automobile industry (4).The energy absorption and mechanical properties of braided composites can be tailored by changing the braid angle; an increase in braid angle leads to an increase in strain to failure and a decrease in stiffness (5). There been several studies reported in literature with regard to effect of braid angle upon the energy absorption of both biaxial and triaxial tubular braided composites under crushing mode (1, 6-8) showing an increase in energy absorption with an increase in braid angle for biaxial braided tubes with the converse for triaxial braided tubes where lower braid angles produce higher energy absorption.

While there have been several works reported in literature with respect to energy absorption properties of braided composites under crushing mode there has been limited work reported in literature for braided composites under tension. The work conducted in (9, 10) to determine the effect of tow continuity for flat braided composites have reported for 45° braid angle where an increase in tensile strength of 20% and a decrease of energy absorption for cut edged specimen with no tow continuity in comparison with uncut edged specimens with tow continuity. The study conducted in (11) on performance of braided composites produced by flattening of biaxial braided sleeves for 25 and 45° braided specimen reported higher tensile strength for 25° braided specimen and the effect of tow continuity was determined to be significant where cut edged specimen depicted lower energy absorption than an uncut edged specimen. The effect of axial tow insertion to produce triaxial tubular braided composites have been studied in (12) where effect of axial tow insertion on axial modulus has been reported to increase only upto 25° braid angle as the axial tows help in stiffening the structure in axial direction.

This paper aims to study the energy absorption and mechanical performance of braided composites in tension by varying braid angle, tow boundary conditions and effect of axial tow insertion.

2. EXPERIMENTAL METHODS

Figure 1 depicts process followed for the experimental method. In order to produce flattened braided composites, cylindrical mandrel with diameter of 2.54 mm was overbraided using a 48 carrier braiding machine at the University of Manchester. Commercially available carbon fibres T700 with 12000 filaments in a tow with individual filament diameter of 7 micro meter from Torayca were used for the producing braided preforms. All 48 carriers were used to produce the braided sleeves leading to regular braid topology (2/2) which implies a tow undulating over and under two tows.

During initial trials the biaxial braided sleeve could not be taken off the mandrel at higher braid angles of 50^0 and 60°; however, at lower angles of 30^0 and 40°, the sleeve could be taken off in a stable tubular state, but there were distortions in the braid angle along the length. Consequently, triaxial braids were produced from which the axial tows were removed that helped in the removal of the braid without any distortions. The probable reason for the stable removal of the braided sleeve using this technique could be that once the axial tows are removed from the braid, gaps are created that help in loosening the tight grip of the braid on the mandrel.

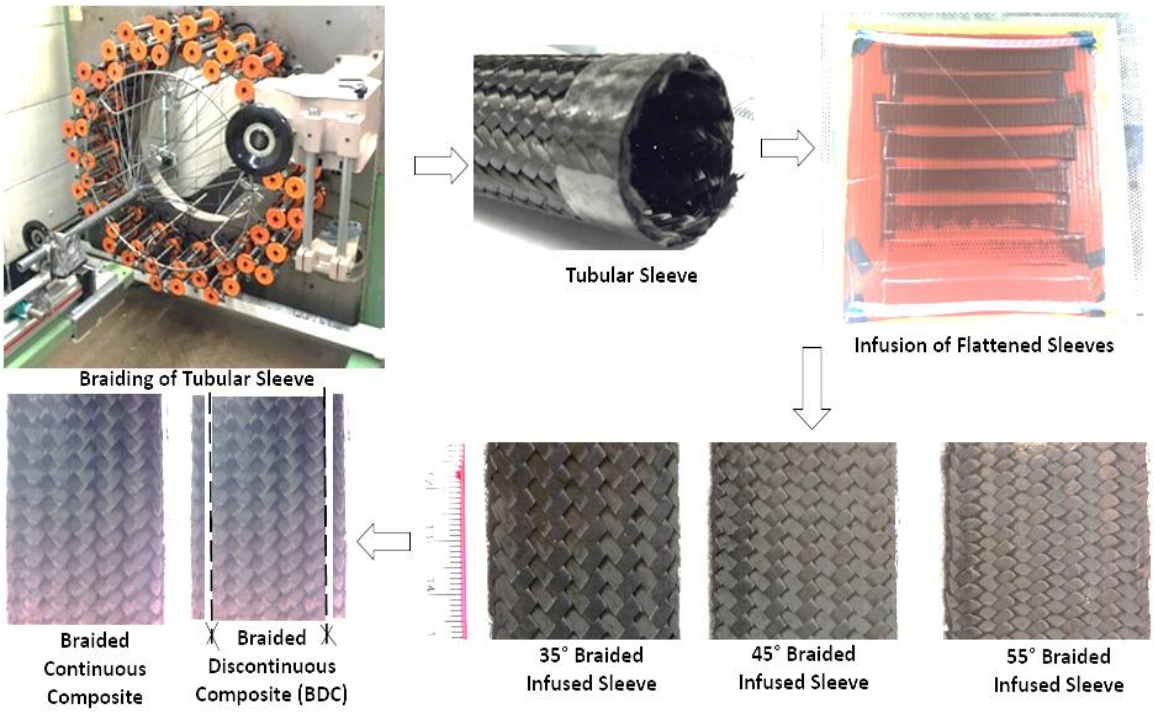

Figure 1: Process followed for producing continuous and discontinuous braided composite coupons.

The braided specimens were taped tightly along the circumference at both ends while still on the mandrel to secure the edges in order to make sure that the perimeter of the cross-section did not change when the specimens were flattened. The tubular braided sleeve was flattened under 20N uniform compression which caused a change in the braid angle; these changes were carefully recorded and have been presented in
Table 1.

Braid Angle on mandrel [^{0}]	Braid Thickness [mm]	Flattened Width Secured Edges [mm]	Braid Angle On flattening with secured edge [^{0}]
25 ± 0.7	1.6 ± 0.6	39.3 ± 0.1	29.6 ± 1.7
30 ± 0.8	1.7 ± 0.6	39.2 ± 0.2	35 ± 1.1
45 ± 1.2	1.8 ± 0.2	38.5 ± 0.5	45 ± 1.7
60 ± 0.3	2.1 ± 0.7	37.4 ± 0.6	55 ± 0.8
65 ± 0.9	2.2 ± 0.4	37.4 ± 0.8	60.7 ± 0.7

Table 1: Change in Braid Angle upon flattening tubular braided sleeve.

As observed in Table 1 the tubes with braid angles below 45° depict increase in braid angle of about 5° however for tubular sleeve with braid angles greater than 45° a converse trend was observed where the braid angle decreased by 5°. However a negligible change in braid angle was observed for 45° braid. Such changes in braid angle when flattening a braided tubular sleeve have not been observed before and further work is required to understand the phenomenon. Triaxial braids were also manufactured using 6 and 12 axial tows inserted in a 45^0 braid, ensuring that the tows were equidistant from each other and were taken off the mandrel without any distortion in the braid angle. In contrast, with biaxial braids, the triaxial braids showed no change in braid angle from tubular to flattened state.

The flattened biaxial and triaxial braided sleeves were then infused using vacuum bag assisted resin infusion with epoxy resin Araldite LY564. The resin-infused sleeves under vacuum were cured at 80°C for 2 hours and post cured at 140°C for 8 hours. After infusion with resin and curing of the composites, the change in braid angle observed from preform to cured state for all types of braids produced was observed to be negligible. In order to determine the effect of braid angle, 5 specimens of each braid angle of 35, 45 and 55° were produced and tested. An additional 5 flattened braided sleeves were produced for each type of braid angle of 35, 45 and 55° and tested with cut edges in order to determine the effect of tow continuity which upon curing were cut by 5mm along both edges containing four interlaced tows. Five specimens of each type of triaxial braided specimens were also produced. The tensile tests were carried out in accordance with ASTM D3158 (13).

Biaxial braided specimens have been labelled BC (braided continuous sleeve) and BDC (braided discontinuous sleeve). BC and BDC are then followed by the braid angles of 35, 45 or 55 ^{0}. The two types of triaxial braids produced were labelled BT0645 and BT1245, with the former implying 45 degree braided triaxial with 6 axial tows and the latter implying 45 degree braided triaxial with 12 axial tows.

3. RESULTS AND DISCUSSION
3.1. FIBRE VOLUME FRACTION AND CRIMP DETERMINATION

Five specimens of each type of braid were examined for their fibre volume content and the fibre volume fraction values for three braid angles (35^0, 45^0 and 55^0) were 0.55, 0.54 and 0.54 as depicted in Table 2 respectively. ASTM D3171 (14) was used to determine the fibre content in the composite using chemical digestion of the matrix. The crimp percentage was calculated as the ratio of the difference between the undulated tow length and actual tow length without undulation to the actual tow length without undulation multiplied by 100 (15). The crimp percentage values as depicted in Table 2 increases with braid angle due to greater undulation which is because an increase in braid angle leads to an increase of tow thickness which leads to a corresponding decrease in the tow width.

Specimen Type	Laminate Thickness [mm]	Tow Width [mm]	Tow Thickness [mm]	Fibre Volume Fraction	Crimp [%]
BC35	1.5 ± 0.1	2.8 ± 0.1	0.27 ± 0.02	0.55 ± 0.1	1.5 ± 0.5
BC45	1.7 ± 0.5	2.1 ± 0.1	0.39 ± 0.03	0.54 ± 0.4	3.5 ± 0.2
BC55	2.5 ± 0.1	2.0 ± 0.1	0.44 ± 0.03	0.54 ± 0.1	4.8 ± 0.3
BDC35	1.49 ± 0.7	2.8 ± 0.1	0.27 ± 0.02	0.55 ± 0.1	1.5 ± 0.5
BDC45	1.8 ± 0.1	2.1 ± 0.1	0.39 ± 0.03	0.54 ± 0.4	3.5 ± 0.2
BDC55	2.5 ± 0.3	2.0 ± 0.1	0.44 ± 0.03	0.54 ± 0.1	4.8 ± 0.3
BT0645	1.9 ± 0.4	1.9 ± 0.2	0.41 ± 0.01	0.55 ± 0.2	4.2 ± 0.04
BT1245	2.1 ± 0.3	1.9 ± 0.4	0.41 ± 0.04	0.56 ± 0.1	4.2 ± 0.1

Table 2 : Specimen specifications for biaxial and triaxial braided laminates

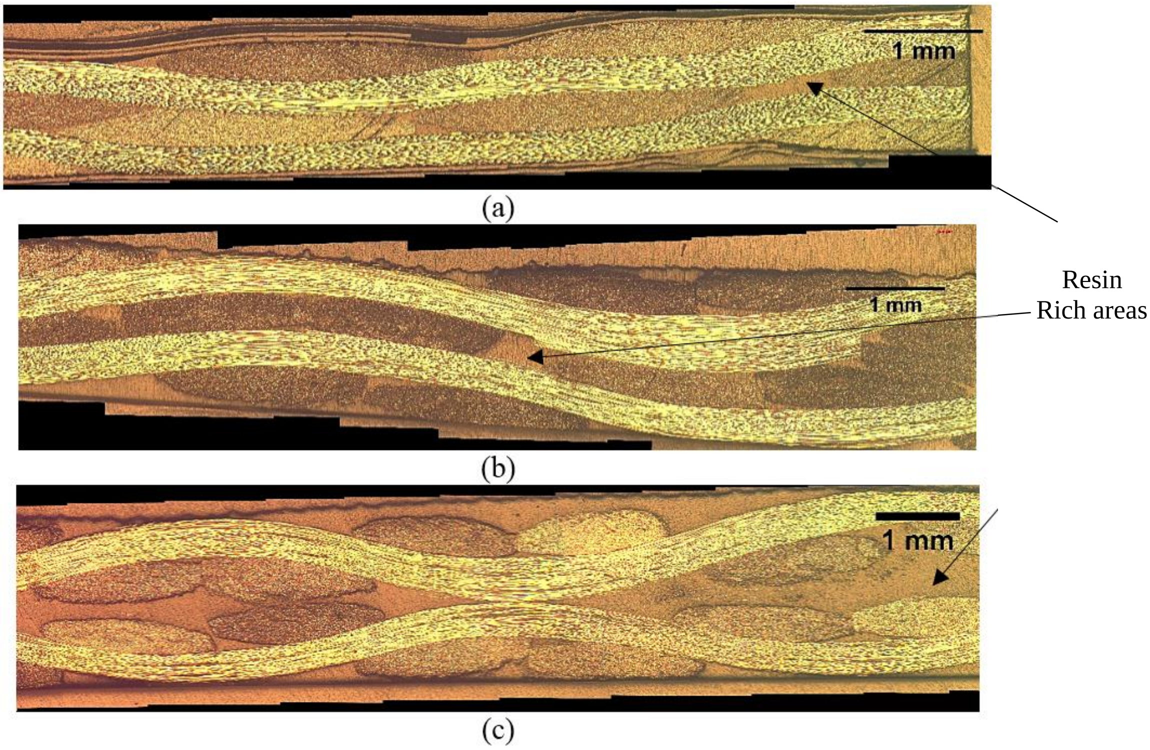

Figure 2: Optical images for braided composites along the fibre axis for (a) 35⁰, (b) 45⁰ and (c) 55⁰

The fibre volume content for triaxial specimen with 6 and 12 axial tows was found to be 0.55 and 0.56 which is a slight increase of 1.8 and 1.9% compared to biaxial braids at same braid angle of 45⁰ as the percentage of fibre increased by 12.5% and 25% by insertion of 6 and 12 axial tows. The triaxial specimen depicted two types of crimp of 3.5% where triaxial tows were not present and 4.2% where triaxial tows were present as depicted in Figure 3.

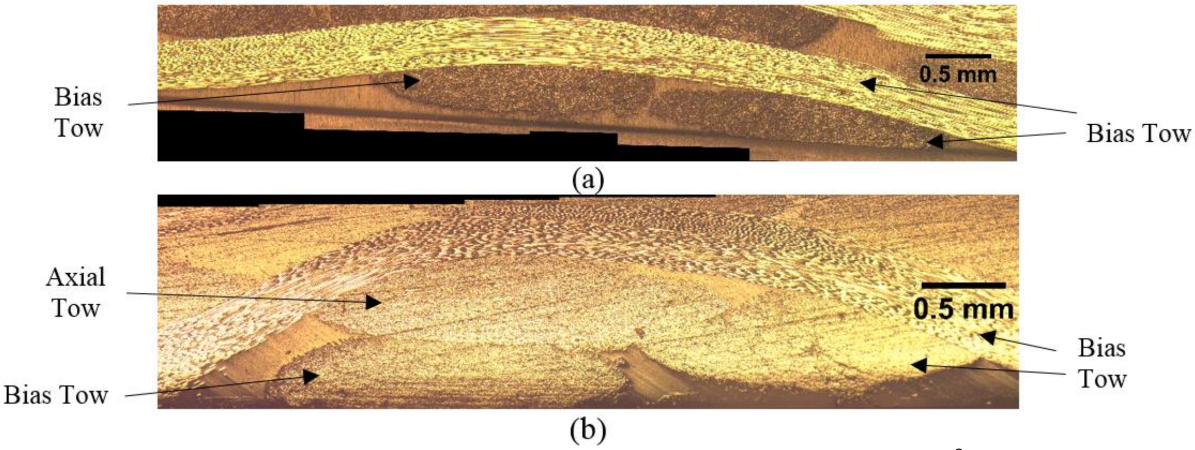

Figure 3: Optical micrographs for braided composites along the fibre axis for 45^0 braided composite for (a) Biaxial, (b) Triaxial braid.

3.2. TENSILE TEST RESULTS

Figure 4 shows typical nominal stress-nominal strain curves for the flattened braided tubes, with cut and uncut edges, for the three braid angles. The effect of braid angle and tow continuity for biaxial braids can be seen in Table 4. For both uncut and cut edged specimens, as the braid angle increased from 35 to 55 ^{0}, the axial strength (ultimate axial stress) and axial modulus decreased. Classic Laminate theory (CLT) was used to predict the modulus of the cross-ply composite laminate that uses properties of unidirectional lamina as the base to describe the stress-strain relationship. The properties of unidirectional lamina were calculated using the Halpin-Tsai equations (16, 17) and presented in the Table 3.

Specimen type	V_f	E_{11} [GPa]	E_{22} [GPa]	G_{12} [GPa]	ν_{12}	ν_{21}
T700	-	230	-	17	0.27	-
LY564	-	2.6	-	0.9	0.25	-
35	0.55	127.6	8.6	2.6	0.25	0.01
45	0.54	125.3	8.4	2.5	0.25	0.01
55	0.54	125.3	8.4	2.5	0.25	0.01

Table 3: Material Properties and Theoretically Calculated Properties for Unidirectional laminate for determining properties of cross-ply laminates using CLT.

The predicted axial moduli values are in reasonable agreement with the measured values for both the cut and uncut specimens (BC and BDC) except for the 45^0 specimens where the measured moduli are about 30 to 40% higher than the predicted moduli; the reasons for this difference are unclear at present. The strain to failure values for both BC and BDC specimens increase with increasing braid angle. The strain to failure for the 35^0 and 45^0 BC specimens is greater than for the BDC specimens. However, for the 55^0 specimens, the strain to failure for the BDC specimens is much greater than for the BC specimens, which relates to the failure mode. The yield stress observed for uncut edged specimens for 35 and 45° braid angles was observed to higher than the uncut edged specimens that had a premature failure as compared to specimens with continuous edges; however the yield stress for cut and uncut edges specimens for 55° braid was observed to be same.

Specimen Type	Axial Modulus [GPa]	Predicted Axial Modulus [GPa]	Ultimate Axial Stress [MPa]	Yield Stress [MPa]	Strain to failure [%]	Specific Energy Absorption [kJ/kg]
T700	230	-	4900	-	2.1	-
LY564	2.6	-	82	-	6.3	-
BC35	22 ±2	21.8	355 ± 40	253 ± 32	12 ± 2	18 ± 2
BC45	13 ± 2	9.6	167 ± 77	135 ± 10	18 ± 2	17± 2
BC55	7 ± 1	7.2	96 ± 8	54 ± 4	39 ± 2	14 ± 1
BDC35	22 ± 1	21.8	317 ± 65	172 ± 29	3 ± 1	3.5 ± 0.2
BDC45	14 ± 2	9.6	197 ± 29	104 ± 11	5 ± 1	5.1 ± 0.4
BDC55	8.2 ± 0.2	7.2	73 ± 11	54 ± 2	54 ± 5	15 ± 2

Table 4: Tensile Properties of Material and Tested specimens.

3.3. NECKING BEHAVIOUR

The stress-strain curves in Figure 4 show significant pseudo-plasticity for many of the specimens. Video recording was carried out for each specimen during the test for macroscopic investigation of the specimens undergoing deformation. For each angle, the BC and the BDC specimens show identical stress-strain behavior initially. At 35^0, whereas the BDC specimens show very little non-linearity before failure, the BC specimens show a peak in the stress-strain curve and significant pseudo-plasticity before failure (about 7%). Similar behavior is seen at 45^0, with a pseudo-plastic strain region of about 12% for the BC specimens. For the 55^0 angle, both the BC and BDC specimens show large regions of pseudo-plasticity of about 35% for the BC specimens and 55% for the BDC specimens.

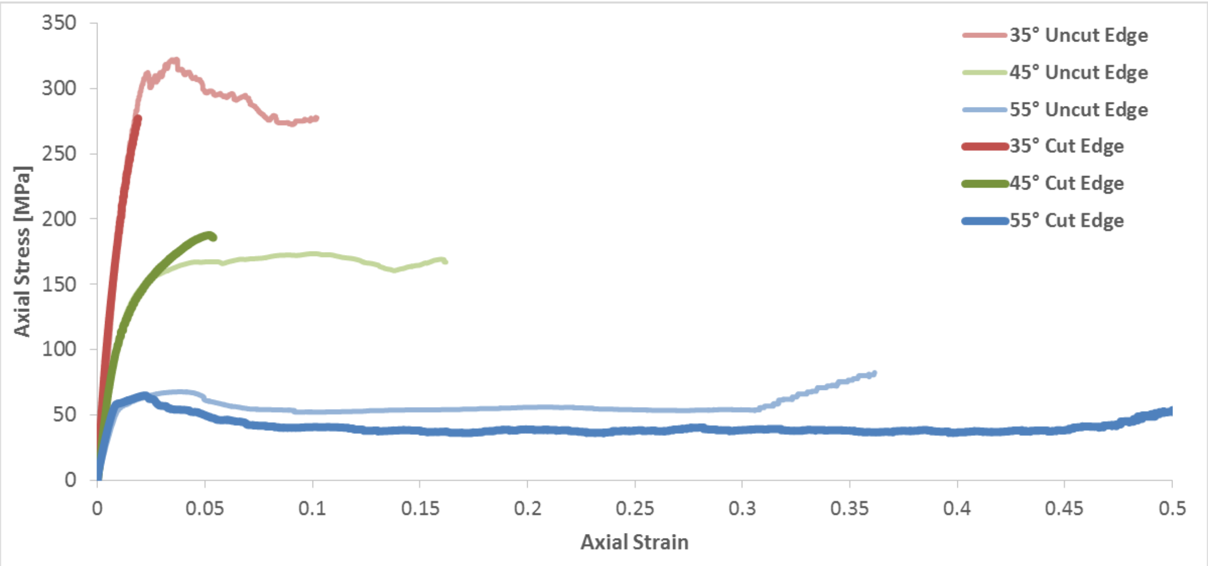

Figure 4: Stress versus strain curves for tested specimens.

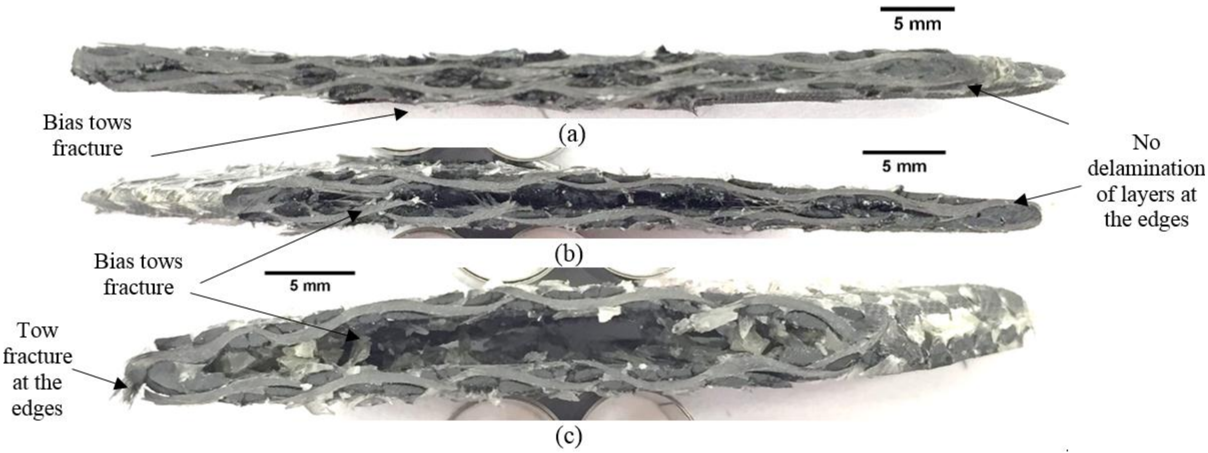

Figure 5: Biaxial Tested specimens with continuous edges (a) 35°, (b) 45°, and (c) 55° braid angles.

Monitoring of the specimens in relation to the stress-strain behavior showed a necking phenomenon for some specimens similar to the necking phenomenon which has been observed previously for braided composite tubes (5). For the BC (i.e. uncut) specimens with braid angles of 35^0 and 45^0, the specimens formed a stable neck in the middle of the coupons which propagated towards the gripped ends of the specimens with increasing strain. As Figure 4 shows, the load fell for the 35^0 specimens as the neck propagated, whereas the load was roughly constant for the 45^0 specimens. For the BDC (cut) specimens with 35^0 and 45^0 angles, there was some slight necking followed by ply delamination and then specimen fracture, with no extensive necking at all.

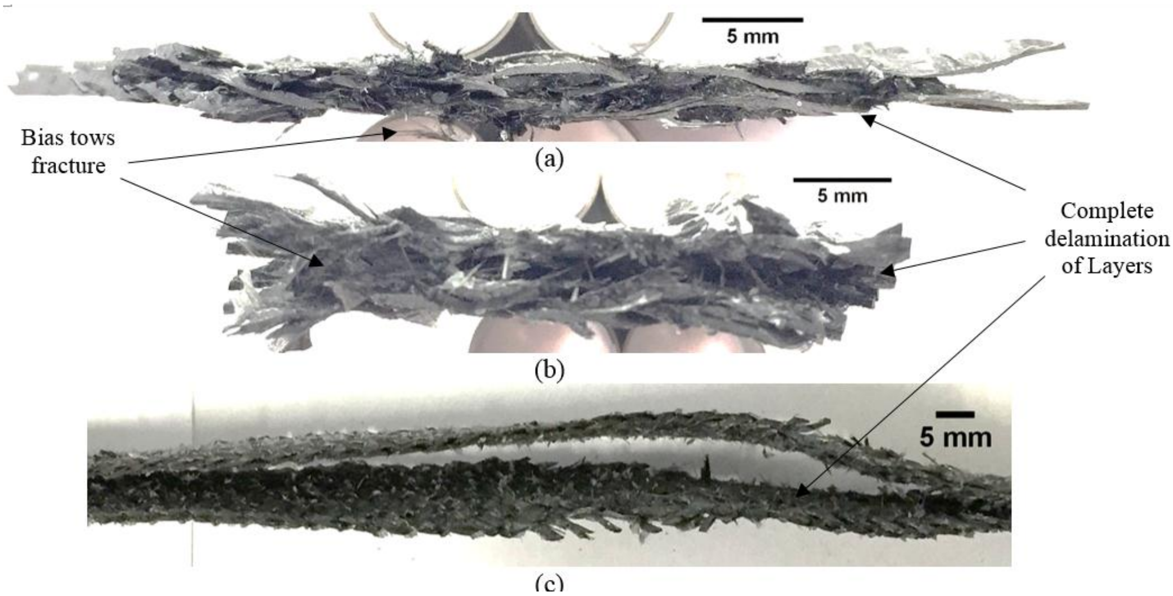

Figure 6: Biaxial Tested specimens with discontinuous edges (a) 35°, (b) 45°, and (c) 55° braid angles.

The 55^0 BC (uncut) specimens showed a similar necking phenomenon to the 35^0 and 45^0 specimens, but with a higher strain to failure. Fractured biaxial tows can be observed in Figure 5 which shows delamination of two layers at failure for three braid angles for uncut specimens which failed along the fibre axis near the tabbing region with minor delamination at the edges. In contrast to all of the other specimens, the BDC (cut) 55^0 specimens failed by a process which consisted of early layer delamination (strain of 0.03) at the edges of the specimen followed by necking of the individual plies which started to develop at one end of the specimen and propagated towards the other end of the specimen. This failure mode produced the highest strain to failure of all the specimens. The 35° braided specimen with dis-continuous edges depicted failure in direction of fibre axis however 45 and 55° braided specimen depicted the failure along the cross-section.

Figure 6 shows complete delamination of layers at all three braid angles investigated. It can be predicted from the sequence of failure for the specimens which showed significant pseudo-plasticity. It was found that matrix failure occurred first, followed by fibre/matrix debonding. The consequence of this combination of failure modes enabled the fibers to reorientate and shear along the loading direction until they reach a locking angle and then fracture. The locking angle was determined from image analysis for the BC specimens with tow continuity. The image analysis revealed that for the BC specimens, locking angles were 30^0, 35^0 and 40^0 for the braid angles of 35^0, 45^0 and 55^0, respectively unlike in [4] where the all braided tubular specimens reached a specific locking angle and ruptured.

3.4. ENERGY ABSORPTION PROPERTIES OF BIAXIAL BRAIDS

The total specific energy absorption was calculated from the area under the stress strain curves. All of the specimens which showed extensive necking to failure absorbed approximately the same specific energy of about 16 kJ/kg. The BC (uncut) specimens values were between 18 and 14 kJ/kg (with the 35^0 specimens showing the highest value and the 55^0 specimens showing the lowest value) and the BDC (cut) 55^0 specimen, which also showed extensive necking after delamination, absorbed about 15 kJ/kg. By contrast, the specimens which failed with very little pseudo-plasticity (BDC35 and BDC45) had the much lower specific energy absorption value of about 4 kJ/kg.

3.5. EFFECT OF AXIAL TOW INSERTION

To investigate the possibility of improving the axial properties of the flattened braided tubular specimen whilst retaining the energy dissipation characteristics associated with the pseudo-plasticity and the necking, triaxial braided 45^0 specimens were manufactured with axial tow insertions of 6 or 12 axial tows.
Figure 8 shows a comparison of typical stress-strain curves for the 45^0 specimens with and without the tow insertions. Specimens with 12 axial tows show a significantly higher axial modulus and tensile strength than the original 45^0 braided specimens, but a much lower strain to failure. The specimens with 6 axial tows show a significantly improved modulus (compared to specimens without the axial tows) and an improved tensile strength, whilst retaining significant pseudo-plasticity. The prediction for axial modulus was carried out for triaxial braided specimens using Halpin-Tsai equations (16, 17). While predicted axial modulus for specimen with 0 and 6 triaxial specimen showed lower values as compared to tested specimens the predicted axial modulus for triaxial specimen with 12 axial tows depicted higher values as compared to experimentally found values. A comparison of the mechanical properties, including the specific energy absorption, is shown in Table 5. The cross-sections of the failed specimens along the fibre axis are shown in Figure 9.

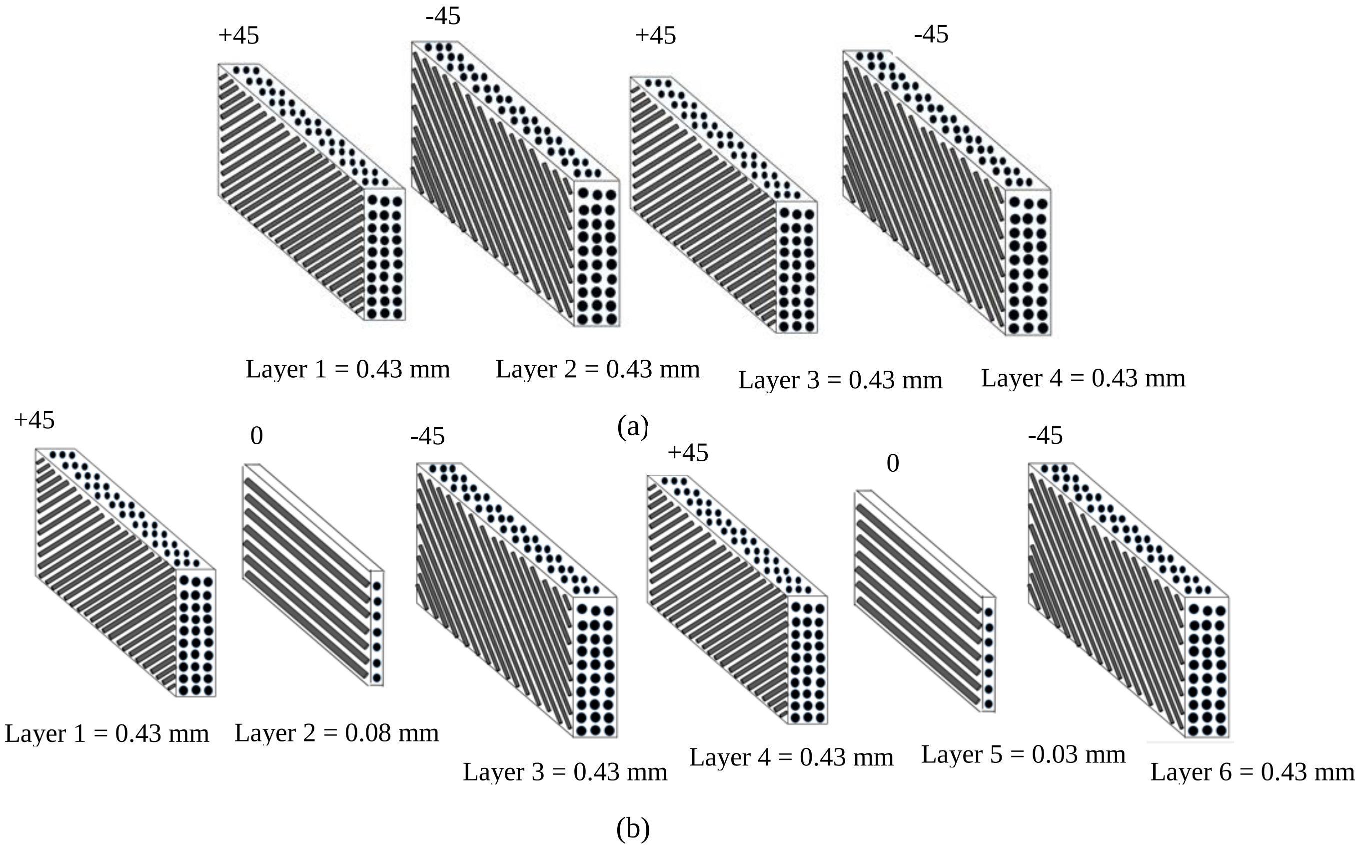

Figure 7: Schematic representation of individual plies for a)$[+45/-45]_s$ and b) $[+45/0/-45]_s$ used to predict axial modulus using CLT.

Specimen Type	Axial Modulus [GPa]	Predicted Axial Modulus [MPa]	Ultimate Axial Stress [MPa]	Yield Stress [MPa]	Strain to failure [%]	Specific Energy Absorption [kJ/kg]
BC45	13 ± 2	9.6	167 ± 77	135 ± 10	18 ± 2	17 ± 2
BT0645	19 ± 2	17.3	195 ± 31	169 ± 35	8 ± 2	9 ± 3
BT1245	22 ± 1	26.4	249 ± 31	-	1.3 ± 0.7	1.8 ± 0.3

Table 5 : Comparison of mechanical properties of 45^0 specimens with and without axial tow insertions.

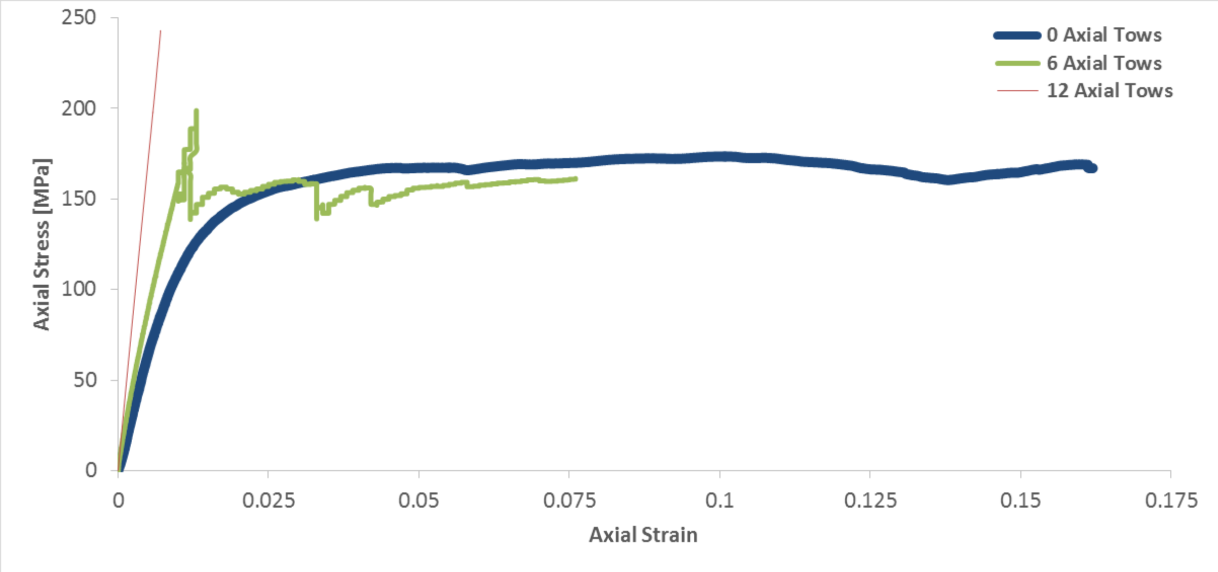

Figure 8: Stress versus strain curves for 45^0 specimens with and without axial tow insertions.

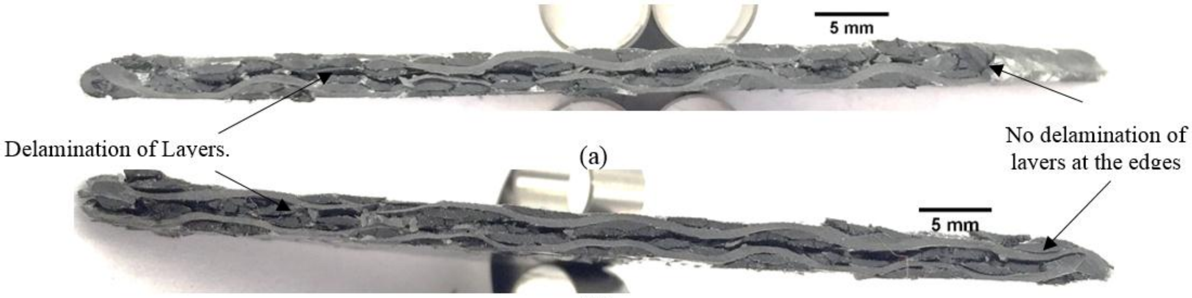

Figure 9: Triaxial Tested specimens for 45⁰ braided specimens with (a) 6 Triaxials and (b) 12 Triaxials

As observed in Table 5 the specimens with 12 axial tows did not depict any yielding while the specimens with 6 and no axial tows depicted yielding. As a consequence of retaining some pseudo-plasticity, the specific energy absorption of the 45^0 specimens with 6 inserted axial tows is about 60% of the value of specimens without axial tows, with an approximately 50% higher axial modulus and an approximately 20% increase in tensile strength. The pseudo-plastic behavior was not observed for 45° specimen with 12 triaxial tows.

4. CONCLUDING REMARKS.

From the experimental work conducted, it can be inferred that braid angle and tow continuity have a significant effect upon the tensile behaviour of flattened tubular braided composites with braid angles in the range 35^0 to 55^0. The biaxial braided specimens with tow continuity throughout the length showed higher axial strains to failure as a consequence of pseudo-plastic behaviour and necking compared to specimens with cut edges (i.e. no tow continuity). However the increasing strain to failure values did not contribute to an increase in specific energy absorption which was approximately the same for all specimens. For 55° biaxial braided specimens with no tow continuity (i.e. cut edges), the axial moduli and failure stresses were approximately the same as for the specimens with continuous edges for the same braiding angle. However, no pseudo-plasticity was observed for the 35^0 and 45^0 braided angle specimens, leading to a low specific energy absorption; for the 55^0 specimens, extensive delamination enabled necking to occur in each layer of the composite which led to high values of both the strain to failure and specific energy absorption. Consequently, these preliminary experiments have shown that triaxial braids incorporating axial insertions can provide a 50% increase in axial modulus and a 20% increase in tensile strength, whilst still retaining 60% of the specific energy absorption through the retention of significant pseudo-plasticity. However, when the number of axial insertions is too high, the braided tubes do not show pseudo-plasticity giving lower specific energy absorption values.

ACKNOWLEDGEMENTS

This work was supported by the Engineering and Physical Sciences Research Council [grant number: EP/IO33513/1], through the EPSRC Centre for Innovative Manufacturing in Composites (CIMComp).

REFERENCES

1. Hull D. A unified approach to progressive crushing of fibre-reinforced composite tubes. Composites Science and Technology. 1991;40(4):377-421.
2. Pizhong Qiao, Mijia Yang, Bobaru F. Impact Mechanics and High-Energy Absorbing Materials: Review. Journal of Aerospace Engineering. 2008;21(4):235–48.
3. Hamada H, Nakai A, Saito H, Sugimoto K, Okano M. Effect of the braiding angle on the energy absorption properties of a hybrid braided FRP tube. Proceedings of the Institution of Mechanical Engineers, Part L: Journal of Materials: Design and Applications. 2005;219(1):59-66.
4. Beard S, Chang FK. Design of Braided Composites for Energy Absorption. Journal of Thermoplastic Composite Materials. 2002;15(1):3-12.
5. Harte A-M, Fleck N. On the mechanics of braided composites in tension. European Journal of Mechanics - A/Solids. 2000;19(2):259-75.
6. Inai R, Chirwa EC, Saito H, Uozumi T, Nakai A, Hamada H. Experimental investigation on the crushing properties of carbon fibre braided composite tubes. I J Crash. 2003;8(5):513-21.
7. Farley GL, Jones RM. Prediction of the energy-absorption capability of composite tubes. Journal of composite materials. 1992;26(3):388-404.
8. Chiu CH, Tsai KH, Huang WJ. Effects of Braiding Parameters on Energy Absorption Capability of Triaxially Braided Composite Tubes. Journal of Composite Materials. 1998;32(21):1964-83.
9. Shinyama Y, Hatsukade Y, Tanaka S, Takai Y, Aly-Hassan MS, Nakai a, et al. Prediction of Initiation Site of Destruction of Flat Braided Carbon Fiber Composites Using HTS-SQUID Gradiometer. Physics Procedia. 2012;36:150-5.
10. Hatsukade Y, Shinyama Y, Yoshida K, Takai Y, Aly-hassan MS, Nakai A, et al. Nondestructive evaluation of ± 45 ° flat-braided carbon-fiber-reinforced polymers with carbon nanofibers using HTS-SQUID gradiometer. Physica C Super Conductivity 2012:2-8.
11. Pickett AK, Fouinneteau MRC. Material characterisation and calibration of a meso-mechanical damage model for braid reinforced composites. Composites Part A: Applied Science and Manufacturing. 2006;37(2):368-77.
12. Xu L, Kim SJ, Ong CH, Ha SK. Prediction of material properties of biaxial and triaxial braided textile composites. Journal of Composite Materials. 2012;46:2255-70.
13. ASTM. Standard Test Method for In-Plane Shear Response of Polymer Matrix Composite Materials by Tensile Test of a ± 45° Laminate. 2001.
14. ASTM. Standard Test Methods for Constituent Content of Composite Materials. 1999.
15. Behara B. HP. Woven Textile Structure: Theory and Applications. Cambridge: Woodhead Publishing in Textiles; 2010.
16. D.Hull, T.W.Clyne. An Introduction to Composite Materials. Second ed: Cambridge University Press; 1996.
17. J.C.Halpin, S.W.Tsai. Environmental Factors in Composite Design. 1967.